Journal of the Brazilian Society of Mechanical Sciences and Engineering (2021) 43:254
https://doi.org/10.1007/s40430-021-02972-z

TECHNICAL PAPER

Buckling analysis of functionally graded beams with periodic nanostructures using doublet mechanics theory

Ufuk Gul[1] · **Metin Aydogdu**[1]

Received: 29 November 2020 / Accepted: 31 March 2021 / Published online: 11 April 2021
© The Brazilian Society of Mechanical Sciences and Engineering 2021

Abstract
Buckling analysis of functionally graded (FG) nanobeams is examined using doublet mechanics theory. The material properties of FG nanobeams change with the thickness coordinate. A periodic nanostructure model is considered in FG nanobeams which has a simple crystal square lattice type and Euler–Bernoulli beam theory is used in the formulation. Softening or hardening material behaviour has been observed by changing chiral angle of the considered FG periodic nanobeams in the present doublet mechanics theory. Unlike other size dependent theories such as nonlocal stress gradient elasticity theory, couple stress theory, strain gradient theory, this mechanical response (softening or hardening) is seen for the first time in doublet mechanics theory. Mechanical material responses are directly affected by the atomic structure of the considered material in the doublet mechanics theory. Firstly, micro-stress and micro-strain relations are obtained for the considered nanostructure model in doublet mechanics theory. Then, these microequations are transformed to macroequations in the present doublet mechanics theory. Thus, more physical and accurate mechanical results can be obtained in nanostructures using the doublet mechanics theory. After developing the mathematical formulations of FG periodic nanobeams, Ritz method is applied to obtain the critical buckling loads for different boundary conditions. Comparison of example studies with the present doublet mechanics model is presented for verification, and effects of chiral angle on stability response of periodic FG nanobeams are discussed.

Keywords Buckling · Doublet mechanics · Functionally graded nanobeams · Hardening · Softening

1 Introduction

Recently, nanotechnology has been commonly used to create new size dependent devices as part of nanoelectromechanical systems such as FG nano/microstructures. FG nanostructures consist of a combination of two different materials which are generally metal and ceramic phases. By use of these FG nanostructures can reduce the stress concentration and thermal stresses at intersection with free surfaces [1]. Considering advantages of these FG nanostructures, many studies have been published about the static and dynamic analyses of FG nanostructures in the literature. Miyamoto et al. [2] investigated the fabrication of FG materials with their application of microstructure analysis. In another study, an analytical solution was developed for FG beams subjected to transverse loads [3]. The elasticity modulus of the FG beam is assumed to change along the thickness coordinate and stresses and displacements were obtained based on Euler–Bernoulli beam model in that paper. Chakraborty et al. [4] studied the thermoelastic behaviour of FG beams using a new beam finite element formulation. Static and dynamic analyses have been presented to investigate the behavioural difference of FG beams. Wattanasakulpong et al. [5] investigated thermal buckling and vibration of the FG beams. They used an approximate Ritz method in the solution. Moreover, there are some important papers related to static and dynamic analyses of FG beams [6–11].

The application of FG beams in nano/microstructures has attracted in the last decade. Hasanyan et al. [12] examined the pull-in instability in FG micromechanical systems considering the Joule's heating. Then, free vibration analysis of FG carbon nanotubes was studied using Timoshenko beam theory [13]. Natural frequencies of FG carbon nanotubes

Technical Editor: Aurelio Araujo.

✉ Ufuk Gul
ufukgul@trakya.edu.tr

[1] Department of Mechanical Engineering, Trakya University, Edirne 22030, Turkey

were found via differential quadrature method. Eltaher et al. [14] investigated the vibration analysis of FG nanobeams based on finite element method. Differential type of nonlocal elasticity theory has been used and equations of motion of FG nanobeams were derived from Hamilton's principle in that paper. After this, Şimşek and Reddy [15] investigated the static buckling of a functionally graded microbeam embedded in an elastic medium based on modified couple stress theory. They focused on the effects of length scale parameter and aspect ratio on the critical buckling loads in detail. Free vibration analysis of FG microbeams was studied via strain gradient Timoshenko beam theory by Ansari et al. [16]. Akgöz and Civalek [17] investigated the free vibration response of axially FG tapered microbeams using the size-dependent modified couple stress theory. Natural frequencies of FG microbeams have been found by the Ritz solution method for clamped-free boundary condition. In another study, stability of FG microbeams was investigated based on the strain gradient theory by the same authors [18]. Stability and dynamic analyses of axially FG microbeams have been investigated by using modified continuum model based on Euler-Bernoulli beam theory in [19]. Eltaher et al. [20] studied the bending and vibration of FG porous nanobeams based on Euler–Bernoulli beam theory. They developed a finite element formulation for FG porous nanobeams in that paper. Recently, Esen et al. [21] examined the vibration of FG cracked microbeam rested on elastic foundation. Thermal and magnetic fields have been considered in the solution. Furthermore, there are some important papers related to static and dynamic analyses of FG beams [22–24].

In most of the papers related to static and dynamic analyses of FG micro/nanobeams, several size dependent continuum theories have been used like a differential type of nonlocal elasticity [25], strain gradient theory [26], couple stress theory [27] and energy equivalent method [28–31]. These size dependent continuum models give acceptable results for mechanical analysis of micro-nanostructures. However, these models predict only one type of mechanical response such as softening or hardening material behaviour. For example, nonlocal differential type elasticity theory predicts softening material behaviour, whereas strain type gradient theory predicts the hardening material behaviour according to the classical elasticity theory. However, it is known that mechanical behaviours of nano/micro-materials directly change with the atomic structure of the materials. Fortunately, a scale dependent theory is called as doublet mechanics (DM) predicts softening or hardening material response depending on the atomic structure of the considered material like experimental studies. Also, the bond length of atoms in the considered material is directly taken as length scale parameter in DM theory. Thus, DM considers the discreteness of the atomic structure of the nano-scale materials. This makes the DM more physical theory than other size dependent theories. DM theory has been firstly identified by Granik [32]. Analytical solutions of nonlinear stability and vibration of imperfect and curved carbon nanotubes have been obtained by using DM theory in [33, 34]. Beside these studies, DM model has been applied to investigate the static and dynamic analyses of nanostructures [35–39].

The essential aim of the present study is to examine the buckling analysis of FG nanobeams considering DM theory. FG nanobeam has been modelled as a simple periodic square crystal lattice structure based on Euler–Bernoulli beam theory in the present study. After deriving mathematical formulations of the FG periodic nanobeam model, stability analysis has been executed by using an approximate Ritz solution method. The effects of chiral angles and power-law indices on the buckling problem of FG nanobeams are investigated. It is notable that softening or hardening mechanical responses occur depending on the chiral angle of the FG periodic nanobeam model in the present DM theory and this important mechanical response can be also seen in experimental studies of nanostructures. Justifying the hardening and softening material behaviours of nano/microstructures may provide a significant advantage to designers. The results obtained from this work can be used in various nano-scale devices such as atomic force microscopes, biosensors, nano-actuators and nano-electromechanical-systems (NEMs).

2 Theory and mathematical formulation

It is seen that bottom surface ($z=-h/2$) of the FG beam is made from metals and top surface ($z=h/2$) is made from ceramics as demonstrated in Fig. 1.

Here, a simple power-law function is recognized to define the variation of the elasticity modulus (E) of FG nanobeam which varies along the thickness coordinate (z) [40]:

$$E(z) = \left(E_c - E_m\right)\left(\frac{z}{h} + \frac{1}{2}\right)^k + E_m \tag{1}$$

where k represents the power-law indices, E_c and E_m represent the values of ceramic and metal phases of the elasticity modulus of the FG nanobeam, respectively. By considering

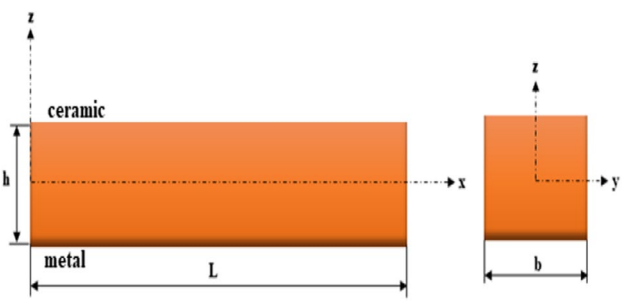

Fig. 1 Functionally graded nanobeam

the DM theory, the strain energy of the nanobeam (U_s) can be determined as [39]:

$$U_s = \frac{1}{2}\int_A \int_0^L \left[\tau_x \cdot \varepsilon_x - \mu_x \cdot \nabla\varepsilon_x\right] \mathrm{d}x\, \mathrm{d}A \tag{2}$$

Here, L is the length, A denotes the cross-sectional area, ε_x and τ_x are the axial macro-strain and shear stress according to the x-axis, respectively. where

$$\nabla\varepsilon_x = \mathrm{d}\varepsilon_x/\mathrm{d}x, \quad \tau_x = E\varepsilon_x, \quad \mu_x = \frac{\eta^2}{12}E\frac{\mathrm{d}\varepsilon_x}{\mathrm{d}x}. \tag{3}$$

Then, by utilizing Eqs. (2) and (3), the strain energy can be written as [39]:

$$U_s = \frac{1}{2}\int_0^L \mathrm{EI}\left[\left(\frac{\partial^2 w}{\partial x^2}\right)^2 - \frac{\eta^2}{12}\left(\frac{\partial^3 w}{\partial x^3}\right)^2\right] \mathrm{d}x \tag{4}$$

Here, E represents the elasticity modulus, w represents the transverse displacement, I represents the second moment of inertia of the rectangular beam cross section and η represents the length scale parameter for the DM theory. In the present study, the second moment of inertia is equal to $I = bh^3/12$, where b is the width and h is the thickness of the beam. Then, potential energy of the external axial load (P) can be defined as follows

$$V = -\frac{1}{2}\int_0^L P\left(\frac{\partial w}{\partial x}\right)^2 \mathrm{d}x \tag{5}$$

For the present study, we consider a periodic nanobeam model. Thus, the strain energy U_s in Eq. (4) can be re-expressed as follows:

$$U_s = \frac{1}{2}\int_0^L \mathrm{EI}\left[f_1(\theta)\left(\frac{\partial^2 w}{\partial x^2}\right)^2 - \frac{\eta^2}{12}f_2(\theta)\left(\frac{\partial^3 w}{\partial x^3}\right)^2\right] \mathrm{d}x \tag{6}$$

where $f_1(\theta)$ and $f_2(\theta)$ represent the direction cosines which depend on the chiral angle (θ) of the atomic structure in the nanobeam. The chiral angle (θ) in a periodic nanobeam takes a value between 0° and 30°. In this study, simple square crystal lattice structure of the periodic nanobeam is taken into account (Fig. 2) and for this lattice type, $f_1(\theta)$ and $f_2(\theta)$ are defined as follows:

$$\begin{aligned} f_1(\theta) = {} & (\cos(\theta))^4 + \left(\cos\left(\tfrac{\pi}{2}+\theta\right)\right)^4 + (\cos(\pi+\theta))^4 + \left(\cos\left(\tfrac{3\pi}{2}+\theta\right)\right)^4 \\ & - \frac{1}{3}\left[(\cos(\theta))^2\left(\cos\left(\tfrac{\pi}{2}-\theta\right)\right)^2 + \left(\cos\left(\tfrac{\pi}{2}+\theta\right)\right)^2(\cos(\theta))^2\right. \\ & \left.+(\cos(\pi+\theta))^2\left(\cos\left(\tfrac{\pi}{2}+\theta\right)\right)^2 + \left(\cos\left(\tfrac{3\pi}{2}+\theta\right)\right)^2(\cos(\theta))^2\right] \end{aligned} \tag{7}$$

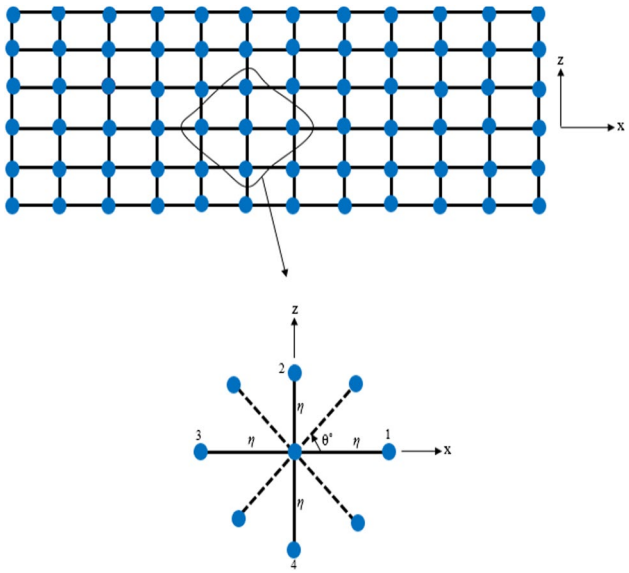

Fig. 2 Arrangement of atoms (nodes) in a periodic nanostructure

$$\begin{aligned} f_2(\theta) = {} & (\cos(\theta))^6 + \left(\cos\left(\tfrac{\pi}{2}+\theta\right)\right)^6 + (\cos(\pi+\theta))^6 + \left(\cos\left(\tfrac{3\pi}{2}+\theta\right)\right)^6 \\ & - \frac{1}{3}\left[(\cos(\theta))^4\left(\cos\left(\tfrac{\pi}{2}-\theta\right)\right)^2 + \left(\cos\left(\tfrac{\pi}{2}+\theta\right)\right)^4(\cos(\theta))^2\right. \\ & \left.+(\cos(\pi+\theta))^4\left(\cos\left(\tfrac{\pi}{2}+\theta\right)\right)^2 + \left(\cos\left(\tfrac{3\pi}{2}+\theta\right)\right)^4(\cos(\theta))^2\right] \end{aligned} \tag{8}$$

We will obtain the critical buckling loads of FG periodic nanobeams in combination of simply supported (**S**), clamped (**C**) and free (**F**) edges of the beam. Accordingly, the geometric and natural boundary conditions (classical and non-classical) are presented as

$$\begin{aligned} & \mathbf{S}: w(x,t) = 0, \\ & \mathrm{EI}\left[f_1(\theta)\left(\frac{\partial^2 w(x,t)}{\partial x^2}\right) + \frac{\eta^2}{12}f_2(\theta)\left(\frac{\partial^4 w(x)}{\partial x^4}\right)\right] = 0, \\ & \frac{\partial^2 w(x)}{\partial x^2} = 0, \quad x = 0, 1. \end{aligned} \tag{9}$$

$$\begin{aligned} & \mathbf{C}: w(x) = 0, \\ & \frac{\partial w(x)}{\partial x} = 0, \\ & \frac{\partial^2 w(x)}{\partial x^2} = 0, \quad x = 0, 1. \end{aligned} \tag{10}$$

$$\begin{aligned}
&\mathbf{F}: \mathrm{EI}\left[f_1(\theta)\left(\frac{\partial^2 w(x)}{\partial x^2}\right)+\frac{\eta^2}{12}f_2(\theta)\left(\frac{\partial^4 w(x)}{\partial x^4}\right)\right]=0,\\
&\mathrm{EI}\left[f_1(\theta)\left(\frac{\partial^3 w(x)}{\partial x^3}\right)+\frac{\eta^2}{12}f_2(\theta)\left(\frac{\partial^5 w(x)}{\partial x^5}\right)\right]=0,\\
&\frac{\partial^2 w(x)}{\partial x^2}=0, \quad x=0,1.
\end{aligned} \tag{11}$$

In this paper, Ritz method will be used to solve the buckling problem of FG periodic nanobeams. In this context, the maximum strain energy of the FG periodic nanobeam can be written as

$$U_{\max}=\frac{1}{2}\int_0^L E(z)I\left[f_1(\theta)\left(\frac{\partial^2 w}{\partial x^2}\right)^2-\frac{\eta^2}{12}f_2(\theta)\left(\frac{\partial^3 w}{\partial x^3}\right)^2\right]\mathrm{d}x \tag{12}$$

Then, based on the Ritz method, the displacement component can be written as [41]:

$$w(x)=\sum_{i=1}^{N}B_i\varphi_i(x) \tag{13}$$

where B_i are unknown coefficients and $\varphi_i(x)$ is the admissible function which satisfies the kinematic boundary conditions. It is assumed that admissible function is written as

$$\varphi_i(x)=X^i, \quad i=1,2,\ldots,N \tag{14}$$

The dimensionless form of algebraic polynomial (X^i) can be determined as below:

$$X^i=\xi^i(\xi-1)^D, \quad \xi=\frac{x}{L}. \tag{15}$$

The values of D in Eq. (15) are equal to $D=0$, 1 and 2 for the free, simply supported and clamped edges, respectively. The total potential energy of FG periodic nanobeams is defined as

$$\Pi=U_{\max}+V \tag{16}$$

Then, substituting Eqs. (14, 15) into Eq. (16) and minimizing Eq. (16) with respect to unknown coefficients (B_i) as below

$$\frac{\partial \Pi}{\partial B_i}=0 \tag{17}$$

Equation (17) gives the following $N\times N$ linear homogeneous equations in an equal number of unknown coefficients B_i. Thus, the standard eigenvalue equation for the buckling of the periodic FG nanobeam can be obtained as

$$\left([K]-\overline{N}[M]\right)\{\Delta\}=0 \tag{18}$$

where $[K]$ is the stiffness matrix, $[M]$ is the geometric stiffness matrix, $\{\Delta\}$ is the column vector of coefficients B_i and $\overline{N}$ is the dimensionless critical buckling load of the FG periodic nanobeam is defined as

$$\overline{N}=\frac{\mathrm{PL}^2}{E_c I} \tag{19}$$

3 Numerical results and discussion

In this section, critical buckling loads of a rectangular cross-sectional periodic FG nanobeam model are shown for different chiral angles, aspect ratio and power-law indices using DM theory. It is assumed that the elasticity modulus of FG beam varies along the thickness direction and two constituents of the elasticity modulus equal to 70 GPa at the bottom surface and 380 GPa at the top surface of FG nanobeam model. Thus, the ratio of the elasticity modulus of the FG periodic nanobeam is taken as $E_{\mathrm{ratio}}=E_{\mathrm{bottom}}/E_{\mathrm{top}}=70/380$ unless otherwise stated in the numerical results. The length scale parameter is taken into consideration as $\eta=0.1421$ nm in the calculations. By considering Ritz method, dimensionless critical buckling loads ($\overline{N}=\mathrm{PL}^2/E_{\mathrm{top}}I$) are found for S–S, C–C, C–F and C–S boundary conditions.

Convergence of the critical buckling loads is presented for different power-law indices in Table 1. It is clearly seen that there is no difference between $N=7$ and $N=8$ terms for S–S, C–C and C–F boundary conditions and critical buckling loads are almost giving same values in case of 7 and 8 terms for the C–S boundary condition. Thus, $N=8$ terms can be acceptable for buckling solution in Ritz method and critical buckling loads will be obtained for $N=8$ in the remaining part of the numerical results.

Some benchmark results are presented in Tables 2 and 3. Present critical buckling loads are compared to the Navier type solution of S–S FG beams [15] for different power-law indices in Table 2. Two models are in a good agreement for all power-law indices. The maximum difference between the two theories is 5.48%. Also, another verification of the present theory can be presented for S–S homogeneous beam with Refs. [9, 15]. Critical buckling loads of S–S homogeneous beams ($\overline{N}=\mathrm{PL}^2/\mathrm{EI}$) have been obtained as 9.87 in [9] and 9.8696 in [15], respectively. By using the same material properties given in [9, 15], the critical buckling load of S–S homogeneous beams has been found as 9.8776 in the present DM theory.

After verification of the present study, Table 3 shows the first three critical buckling loads of periodic FG nanobeams for local elasticity (LE) and DM theories. Here, DM results are given for different chiral angle of the atomic structure of the periodic FG nanobeam. Depending

Table 1 Convergence of the critical buckling loads for different boundary conditions ($L/h=5$, $E_{ratio}=70/380$, $\eta=0.1421$ nm)

N	S–S			C–C			C–F			C–S		
	$\theta=30°$	$\theta=15°$	$\theta=0°$	$\theta=30°$	$\theta=15°$	$\theta=0°$	$\theta=30°$	$\theta=15°$	$\theta=0°$	$\theta=30°$	$\theta=15°$	$\theta=0°$
$k=0$												
6	9.8726	16.4522	19.7420	39.3996	65.6310	78.7467	2.4670	4.1116	4.9339	20.1679	33.6031	40.3206
7	9.8726	16.4521	19.7419	39.3995	65.6309	78.7466	2.4670	4.1116	4.9339	20.1679	33.6030	40.3205
8	9.8726	16.4521	19.7419	39.3995	65.6309	78.7466	2.4670	4.1116	4.9339	20.1678	33.6028	40.3203
$k=0.5$												
6	7.1880	11.9784	14.3736	28.6857	47.7840	57.3315	1.7962	2.9935	3.5922	14.6837	24.4654	29.3562
7	7.1879	11.9783	14.3734	28.6856	47.7839	57.3330	1.7962	2.9935	3.5922	14.6836	24.4653	29.3561
8	7.1879	11.9783	14.3734	28.6856	47.7839	57.3330	1.7962	2.9935	3.5922	14.6836	24.4652	29.3560
$k=2$												
6	4.5033	7.5045	9.0051	17.9717	29.9369	35.9195	1.1253	1.8755	2.2505	9.1994	15.3277	18.3918
7	4.5033	7.5044	9.0050	17.9717	29.9369	35.9195	1.1253	1.8755	2.2505	9.1994	15.3276	18.3918
8	4.5033	7.5044	9.0050	17.9717	29.9369	35.9195	1.1253	1.8755	2.2505	9.1994	15.3275	18.3917

Table 2 Comparison of the critical buckling loads ($\overline{N}=PL^2/E_{top}I$) of S–S FG beams for different power-law indices ($\eta=0$, $L/h=20$, $E_{ratio}=390/210$)

k	Present	[15]
0	18.3441	18.3292
0.2	16.9330	16.5116
1	14.1108	13.3765
2	12.6997	12.5777
5	11.2887	11.8099

on the chiral angle of the simple square crystal lattice structure, DM predicts hardening or softening material behaviour according to LE theory. At $\theta=30°$, DM gives smaller critical buckling loads than LE. However, the reverse is true for $\theta=0°$ and $\theta=15°$. This proves that DM considers the atomic structure of the material like experimental studies. This result is the first reported among the scale-dependent continuum models. The difference between LE and DM theory becomes maximum for $\theta=0°$ and becomes minimum for $\theta=30°$. It is also seen that the difference between both models increases with increasing the mode number for all chiral angles. By increasing the power-law indices (k) critical buckling loads decrease for two theories.

Figure 3 demonstrates the variation of critical buckling load with power-law indices for LE and DM theories. It is remarkable that hardening behaviour occurs when $\theta=0°$ and $\theta=15°$ whereas softening material behaviour occurs when $\theta=30°$ in DM for all boundary conditions. This is because beam stiffness increases or decreases depending on the orientation of simple square crystal lattice structure. DM and LE theory give very close buckling load values for $\theta=30°$. Critical buckling loads decrease with increasing the power-law indices for both theories in all boundary conditions.

4 Conclusions

In this paper, buckling analysis of periodic FG nanobeams is investigated within the framework of DM theory. In order to solve the buckling problem, the Ritz solution method is used. In this context, some remarkable results have been listed as below:

- It is observed that critical buckling loads obtained by DM give smaller (for $\theta=30°$) or higher (for $\theta=0°$, 15°) values than LE depending on the chiral angle of the simple square lattice of the periodic FG nanobeam model.
- This provides crucial advantages to designers to attain the softening or hardening material responses of the micro/nanostructures. This also proves that discreteness of the atomic structure of the considered materials directly is included in DM theory.
- Gradient effects become more significant for the higher modes and hardening material response in DM theory.
- Decrease of the power-law indices increases the critical buckling loads for LE and DM theories.

Table 3 The first three critical buckling loads ($\overline{N} = \mathrm{PL}^2/E_{\mathrm{top}}I$) with $L/h = 10$ and $E_{\mathrm{ratio}} = 70/380$ ($\eta = 0.1421$ nm)

k	Theory		S–S	C–C	C–F	C–S
0	LE ($\eta=0$)	$\overline{N}_1$	9.8776	39.4784	2.4674	20.1907
		$\overline{N}_2$	39.4667	80.7629	22.2066	59.6795
		$\overline{N}_3$	88.8712	157.9569	61.6861	118.9181
	DM ($\theta=30°$)	$\overline{N}_1$	9.8763	39.4587	2.4673	20.1850
		$\overline{N}_2$	39.4667	80.6723	22.2003	59.6329
		$\overline{N}_3$	88.7751	157.6399	61.6382	118.7367
	DM ($\theta=15°$)	$\overline{N}_1$	16.4600	65.7557	4.1121	33.6392
		$\overline{N}_2$	65.7690	134.4136	36.9978	99.3674
		$\overline{N}_3$	147.9158	262.5923	102.7090	197.8137
	DM ($\theta=0°$)	$\overline{N}_1$	19.7519	78.9042	4.9345	40.3663
		$\overline{N}_2$	78.9201	161.2843	44.3965	119.2346
		$\overline{N}_3$	177.4861	315.0685	123.2444	237.3522
0.5	LE ($\eta=0$)	$\overline{N}_1$	7.1915	28.7430	1.7964	14.7002
		$\overline{N}_2$	28.7488	58.8010	16.1679	43.4509
		$\overline{N}_3$	64.7044	115.0037	44.9118	86.5807
	DM ($\theta=30°$)	$\overline{N}_1$	7.1907	28.7287	1.7963	14.6961
		$\overline{N}_2$	28.7345	58.7351	16.1634	43.4169
		$\overline{N}_3$	64.6345	114.7729	44.8769	86.4486
	DM ($\theta=15°$)	$\overline{N}_1$	11.9840	47.8748	2.9939	24.4917
		$\overline{N}_2$	47.8844	97.8626	26.9370	72.3464
		$\overline{N}_3$	107.6930	191.1856	74.7794	144.0223
	DM ($\theta=0°$)	$\overline{N}_1$	14.3807	57.4478	3.5927	29.3895
		$\overline{N}_2$	57.4597	117.4263	32.3238	86.8111
		$\overline{N}_3$	129.2223	229.3920	89.7306	172.8090
2	LE ($\eta=0$)	$\overline{N}_1$	4.5055	18.0076	1.1254	9.2098
		$\overline{N}_2$	18.0113	36.8392	10.1293	27.2222
		$\overline{N}_3$	40.5377	72.0505	28.1375	54.2433
	DM ($\theta=30°$)	$\overline{N}_1$	4.5050	17.9987	1.1253	9.2072
		$\overline{N}_2$	18.0023	36.7979	10.1264	27.2009
		$\overline{N}_3$	40.4939	71.9059	28.1156	54.1606
	DM ($\theta=15°$)	$\overline{N}_1$	7.5081	29.9938	1.8757	15.3442
		$\overline{N}_2$	29.9999	61.3115	16.8762	45.3254
		$\overline{N}_3$	67.4703	119.7789	46.8497	90.2308
	DM ($\theta=0°$)	$\overline{N}_1$	9.0096	35.9914	2.2508	18.4127
		$\overline{N}_2$	35.9986	73.5683	20.2510	54.3877
		$\overline{N}_3$	80.9585	143.7154	56.2167	108.2659

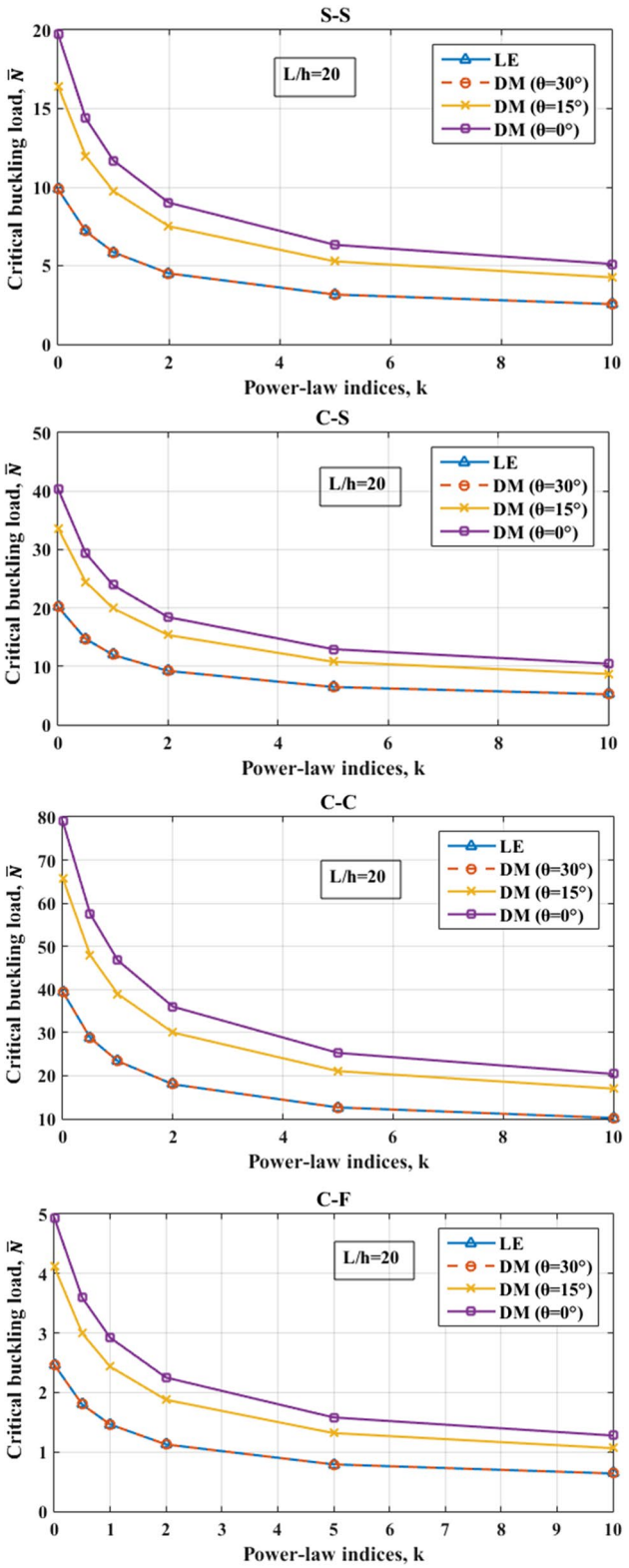

Fig. 3 Variation of the critical buckling load with power-law indices for different boundary conditions

Funding The author received no financial support for the research, authorship, and/or publication of this article.

Declarations

Conflict of interest The authors declare that they have no conflict of interest.

References

1. Şimşek M, Yurtcu HH (2013) Analytical solutions for bending and buckling of functionally graded nanobeams based on the nonlocal Timoshenko beam theory. Compos Struct 97:378–386
2. Miyamoto Y, Kaysser WA, Rabin BH, Kawasaki A, Ford RG (1999) Functionally graded materials: design, processing and applications. Kluwer Academic Publihers, London
3. Sankar BV (2001) An elasticity solution for functionally graded beams. Compos Sci Technol 61:689–696
4. Chakraborty A, Gopalakrishnan S, Reddy JN (2003) A new beam finite element for the analysis of functionally graded materials. Int J Mech Sci 45:519–539
5. Wattanasakulpong N, Prusty BG, Kelly DW (2011) Thermal buckling and elastic vibration of third-order shear deformable functionally graded beams. Int J Mech Sci 53:734–743
6. Aydogdu M, Taskin V (2007) Free vibration analysis of functionally graded beams with simply supported edges. Mater Des 28:1651–1656
7. Li XF (2008) A unified approach for analysing static and dynamic behaviors of functionally graded Timoshenko and Euler-Bernoulli beams. J Sound Vib 318:1210–1229
8. Sina SA, Navazi HM, Haddadpour H (2009) An analytical method for free vibration analysis of functionally graded beams. Mater Des 30:741–747
9. Reddy JN (2011) Microstructure-dependent couple stress theories of functionally graded beams. J Mech Phys Solids 59:2382–2389
10. Nguyen TK, Nguyen BD, Vo TP, Thai HT (2017) Hygro-thermal effects on vibration and thermal buckling behaviours of functionally graded beams. Compos Struct 176:1050–1060
11. Arefi M, Zenkour AM (2017) Wave propagation analysis of a functionally graded magneto-electro-elastic nanobeam rest on Visco-Pasternak foundation. Mech Res Commun 79:51–62
12. Hasanyan DJ, Batra RC, Harutyunyan S (2008) Pull-in instabilities in functionally graded microthermoelectromechanical systems. J Therm Stress 31:1006–1021
13. Janghorban M, Zare A (2011) Free vibration analysis of functionally graded carbon nanotubes with variable thickness by differential quadrature method. Phys E 43:1602–1604
14. Eltaher MA, Emam SA, Mahmoud FF (2012) Free vibration analysis of functionally graded size-dependent nanobeams. Appl Math Comput 218:7406–7420
15. Şimşek M, Reddy JN (2013) A unified higher order beam theory for buckling of a functionally graded microbeam embedded in elastic medium using modified couple stress theory. Compos Struct 101:47–58
16. Ansari R, Gholami R, Sahmani S (2011) Free vibration analysis of size-dependent functionally graded microbeams based on the strain gradient Timoshenko beam theory. Compos Struct 94:221–228
17. Akgöz B, Civalek Ö (2013) Free vibration analysis of axially functionally graded tapered Bernoulii–Euler microbeams based on the modified couple stress theory. Compos Struct 98:314–322

18. Akgöz B, Civalek Ö (2013) Buckling analysis of functionally graded microbeams based on the strain gradient theory. Acta Mech 224:2185–2201
19. Abo-bakr HM, Abo-bakr RM, Mohamed SA, Eltaher MA (2021) Multi-objective shape optimization for axially functionally graded microbeams. Compos Struct 258:113370
20. Eltaher MA, Fouda N, El-midany T, Sadoun AM (2018) Modified porosity model in analysis of functionally graded porous nanobeams. J Braz Soc Mech Sci Eng 40:141
21. Esen I, Özarpa C, Eltaher MA (2021) Free vibration of a cracked FG microbeam embedded in an elastic matrix and exposed to magnetic field in a thermal environment. Compos Struct 261:113552
22. Abo-bakr RM, Abo-bakr HM, Mohamed SA, Eltaher MA (2021) Optimal weight for buckling of FG beam under variable axial load using Pareto optimality. Compos Struct 258:113193
23. Abo-bakr RM, Eltaher MA, Attia MA (2020) Pull-in and free-standing instability of actuated functionally graded nanobeams including surface and stiffening effects. Eng Comput. https://doi.org/10.1007/s00366-020-01146-0
24. Abo-bakr HM, Abo-bakr RM, Mohamed SA, Eltaher MA (2020) Weight optimization of axially functionally graded microbeams under buckling and vibration behaviors. Mech Based Design Struct Mach. https://doi.org/10.1080/15397734.2020.1838298
25. Eringen AC (1976) Nonlocal polar field models. Academic Press, New York
26. Mindlin RD (1964) Micro-structure in linear elasticity. Arch Ration Mech Anal 16:51–78
27. Cosserat E, Cosserat F (1909) Sur la théorie des corps déformables. Herman, Paris (**In French**)
28. Mohamed N, Eltaher MA, Mohamed SA, Seddek LF (2019) Energy equivalent model in analysis of postbuckling of imperfect carbon nanotubes resting on nonlinear elastic foundation. Struct Eng Mech 70(6):737–750
29. Eltaher MA, Mohamed N, Mohamed S, Seddek LF (2019) Postbuckling of curved carbon nanotubes using energy equivalent model. J Nano Res 57:136–157
30. Eltaher MA, Almalki TA, Ahmed KIE, Khalid H (2019) Characterization and behaviors of single walled carbon nanotube by equivalent-continuum mechanics approach. Adv Nano Res 7(1):39–49
31. Mohamed N, Mohamed SA, Eltaher MA (2020) Buckling and post-buckling behaviors of higher order carbon nanotubes using energy-equivalent model. Eng Comput. https://doi.org/10.1007/s00366-020-00976-2
32. Granik VT (1978) Microstructural mechanics of granular media. Technique report IM/MGU Inst Mech Moscow State Univ, pp 78–241
33. Eltaher MA, Mohamed N (2020) Nonlinear stability and vibration of imperfect CNTs by doublet mechanics. Appl Math Comput 382:125311
34. Eltaher MA, Mohamed N, Mohamed SA (2020) Nonlinear buckling and free vibration of curved CNTs by doublet mechanics. Smart Struct Syst 26(2):213–226
35. Ferrari M, Granik VT, Imam A (1997) Introduction to doublet mechanics, Advances in Doublet Mechanics. Springer, Berlin, Heidelberg, pp 1–26
36. Gul U, Aydogdu M, Gaygusuzoglu G (2017) Axial dynamics of a nanorod embedded in an elastic medium using doublet mechanics. Compos Struct 160:1268–1278
37. Gul U, Aydogdu M (2018) Structural modelling of nanorods and nanobeams using doublet mechanics theory. Int J Mech Mater Des 14:195–212
38. Gul U, Aydogdu M (2018) Noncoaxial vibration and buckling analysis of embedded double-walled carbon nanotubes by using doublet mechanics. Compos Part B 137:60–73
39. Gul U, Aydogdu M (2018) Vibration and buckling analysis of nanotubes (nanofibers) embedded in an elastic medium using Doublet Mechanics. J Eng Math 109:85–111
40. Reddy JN (2004) Mechanics of laminated composite plates and shells: theory and analysis. CRC Press, Boca Raton
41. Leissa AW (2005) The historical bases of the Rayleigh and Ritz methods. J Sound Vib 287(4–5):961–978

Publisher's Note Springer Nature remains neutral with regard to jurisdictional claims in published maps and institutional affiliations.